

Angular Distributions for ${}^6\text{Li}(p, \gamma){}^7\text{Be}$

C. I. W. Tingwell,^A J. D. King^{A, B} and D. G. Sargood^A

^A School of Physics, University of Melbourne,
Parkville, Vic. 3052.

^B Permanent address: Department of Physics,
University of Toronto, Toronto, ON M5S 1A7, Canada.

Abstract

Angular distributions of γ rays leading directly to the ground and first excited states in the reaction ${}^6\text{Li}(p, \gamma){}^7\text{Be}$ have been measured at bombarding energies of 500, 800 and 1000 keV. The results are compared with those of previous measurements and substantial agreement is found. The results are also compared with theoretical predictions of a simple direct capture model.

1. Introduction

As a test of the assumption that nucleon direct capture cross sections may be calculated with optical model potentials having the same parameter values for mirror reactions, Switkowski *et al.* (1979) measured the absolute cross sections of ${}^6\text{Li}(p, \gamma_{0,1}){}^7\text{Be}$ over the energy range $E_p = 200\text{--}1200$ keV, and compared their results with the calculations of Barker (1974, 1980) based on parameters chosen to fit the thermal cross section of ${}^6\text{Li}(n, \gamma){}^7\text{Li}$. The agreement was good. However, Barker's model was not unique. He considered nine different sets of potential well parameters (Barker 1980), six of which gave cross sections in reasonable agreement with the experimental data, but which gave significantly different angular distributions. The published experimental angular distribution measurements for ${}^6\text{Li}(p, \gamma){}^7\text{Be}$, those by Warren *et al.* (1956) at $E_p = 750$ keV and the preliminary data by Johnston *et al.* (1969) at $E_p = 800$ keV, were not in strong agreement, so there were no definitive data with which to compare the angular distributions obtained from Barker's calculations and so differentiate between his parameter sets. We therefore decided to make a further measurement of the angular distributions at three different energies including $E_p = 800$ keV, the energy at which Barker listed all his results for each parameter set.

2. Experimental Methods

Target Preparation

Since the Q -values of ${}^6\text{Li}(p, \gamma_0){}^7\text{Be}$ and ${}^6\text{Li}(p, \gamma_1){}^7\text{Be}$ are 5.606 and 5.177 MeV respectively, and since the γ rays from these reactions are subject to Doppler shifts which vary significantly as a function of the angle of observation, it is difficult to find experimental conditions under which the γ rays of interest are not obscured by the 6.130 and 7.117 MeV γ rays from the contaminant reaction ${}^{19}\text{F}(p, \alpha\gamma){}^{16}\text{O}$. It was, accordingly, necessary to ensure that targets were as free of fluorine as possible.

Furthermore, the low melting point of lithium (180°C) made it mandatory that the target be efficiently cooled.

The target preparation procedure consisted of vacuum evaporation of a layer of gold onto the machined flat face of a copper rod of diameter 1.75 cm followed by evaporation of Al onto about one-third of the gold face and of Li metal enriched to 99% in ^6Li onto another third of the gold face. Both evaporations were made from tungsten boats which had previously been outgassed at white heat. The gold, which was of stopping thickness for all protons used in this experiment, provided a fluorine-free backing for the Li, and the Li was in complete thermal contact with the copper rod for cooling purposes. From the width of the full energy peak of direct capture γ rays in the subsequent measurements, the thickness of the Li target was found to be 30 to 800 keV protons. The Al target was used for calibration measurements. It was 13 keV thick to 1 MeV protons, as determined from the full width at half maximum of the 992 keV resonance in $^{27}\text{Al}(p, \gamma)^{28}\text{Si}$. A quartz plate was mounted on the remaining third of the gold face and after partial oxidation of the lithium in air, the whole assembly was transferred to the reaction chamber. The lithium was allowed to oxidise because we had found from previous measurements that this led to a more robust target.

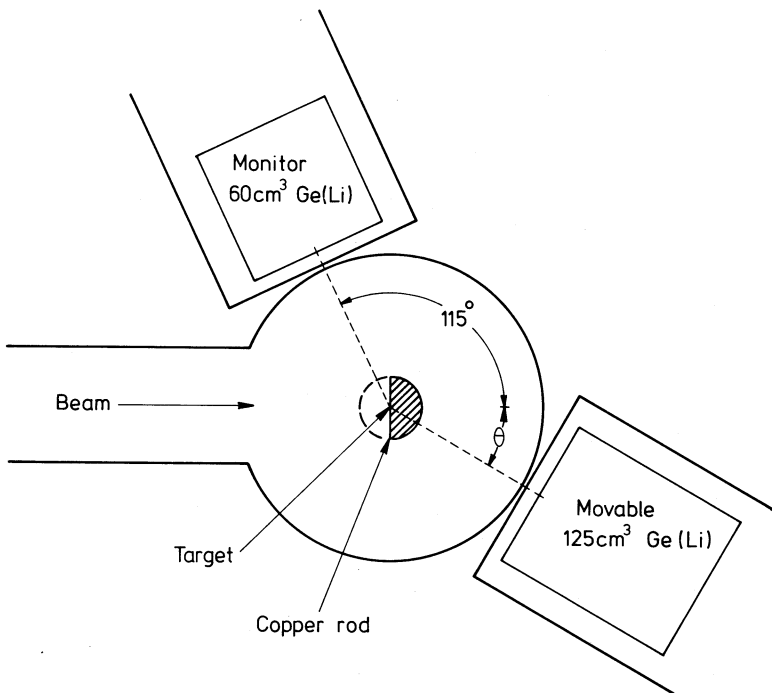


Fig. 1. Detection geometry used for angular distribution measurements.

Detection Geometry

The detection geometry is illustrated in Fig. 1. The target rod was mounted in a stainless steel spherical chamber, with a wall thickness of 1 mm, which was insulated from the beamline and acted as a Faraday cup. The target face was directly above

the axis of a goniometer table which carried the 125 cm³ Ge(Li) detector used to detect the γ rays. After collimation the incident beam passed through an electron suppressor held at -600 V and impinged on the target, with a beam spot diameter of 2 mm. With the beam spot accurately centred, γ rays produced at the target would pass through 9.5 mm of copper and 1 mm of stainless steel to reach the detector at all angles from 0° to 75° and through just 1 mm of stainless steel at backward angles. Only when the detector was at 90° was it necessary to consider the effect of the difference in absorber thickness at forward and backward angles on the effective angle of observation. The face of the detector can cleared the wall of the reaction chamber by 1 mm for all angles of observation from 0° to 120°, which corresponded to a distance of 5.1 cm from the target spot to the face of the detector can. At 120° the edge of the detector just cleared the beamline, but with the detector pulled back to a distance of 6.2 cm from the target spot it was possible to make a measurement at 135°.

A second detector, of active volume 60 cm³, was located on the other side of the chamber at a fixed angle of 115° and 1 mm clear of the chamber wall. This was used as a monitor for the angular distribution measurements: measurement of the yield of γ rays for the angular distribution, relative to the monitor detector yield of γ rays from proton induced reactions on ${}^6\text{Li}$ or ${}^7\text{Li}$, avoids any effects due to possible variations in target thickness or to target deterioration under bombardment.

Details of Angular Distribution Measurements

The bombarding energies at which angular distributions were measured were dictated by the need to avoid ${}^{19}\text{F}(p, \alpha\gamma){}^{16}\text{O}$ resonances, by the need to attempt to keep the ${}^6\text{Li}(p, \gamma_0){}^7\text{Be}$ and ${}^6\text{Li}(p, \gamma_1){}^7\text{Be}$ γ -ray peaks resolved, at all angles of observation, from those arising from ${}^{19}\text{F}(p, \alpha\gamma){}^{16}\text{O}$ even off-resonance, by the requirement of a realistic count rate at the lowest bombarding energy, and by the need to avoid domination by the 1.84 MeV resonance in ${}^6\text{Li}(p, \gamma){}^7\text{Be}$. The bombarding energies chosen were 500, 800 and 1000 keV. The University of Melbourne 5U Pelletron accelerator would not supply stable proton beams of ≥ 10 μA at the required energies, at the time of the experiment, so the measurements were made with beams of ~ 6 μA of H_2^+ ions at energies of 1000, 1600 and 2000 keV.

The target rod passed through the bottom part of the chamber via stainless steel bellows and into a vacuum flask containing ice and water. This provided adequate target cooling and the range of linear motion needed to permit selection of the Al, ${}^6\text{Li}$, or quartz target. The beamline and target chamber were ion pumped to a pressure of $\sim 2 \times 10^{-8}$ Torr (1 Torr \equiv 133 Pa) throughout the experiment to minimise possible build up of ${}^{19}\text{F}$ contamination.

The γ -ray pulse height spectra from both detectors were stored in a PDP 11/40 on-line computer. The angular distributions were measured in 15° steps, the sequence of angles being 0°, 30°, 60°, 90°, 120°, 105°, 75°, 45°, 15° following which the detector was pulled back to the 6.2 cm position and measurements were made at 135°. The charge of H_2^+ ions collected per point was in the range 25–45 mC.

The angular dependence of the detection efficiency was determined from observation of the 1779 and 6020 keV γ rays from the decay of the 992 keV resonance in ${}^{27}\text{Al}(p, \gamma){}^{28}\text{Si}$ which are known to be isotropic to within 2% and 3% respectively (Anttila *et al.* 1977), from observation of the isotropic 478 and 429 keV γ rays from the $\frac{1}{2}^-$ first excited states of ${}^7\text{Li}$ and ${}^7\text{Be}$ [excited by ${}^7\text{Li}(p, p'\gamma){}^7\text{Li}$ and ${}^6\text{Li}(d, p\gamma){}^7\text{Li}$

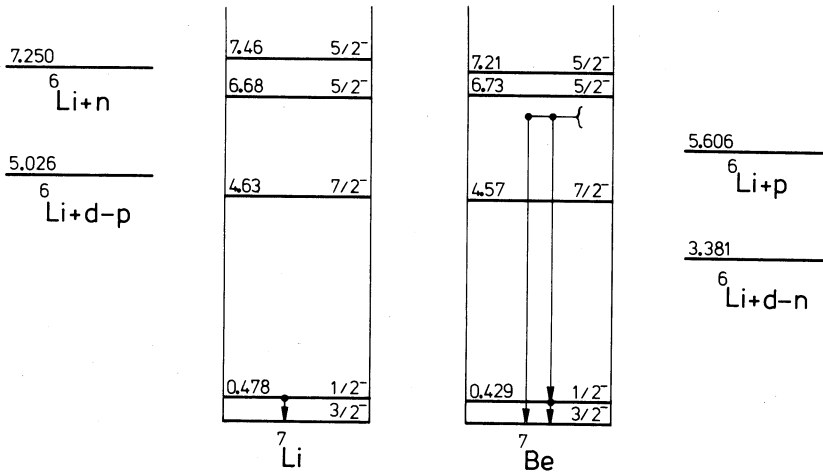


Fig. 2. Partial energy level schemes of ${}^7\text{Li}$ and ${}^7\text{Be}$. The information is taken from Ajzenberg-Selove (1984).

and by ${}^6\text{Li}(p, \gamma){}^7\text{Be}$ and ${}^6\text{Li}(d, n\gamma){}^7\text{Be}$ respectively], and from the 6130 MeV γ ray from the 935 keV resonance in ${}^{19}\text{F}(p, \alpha\gamma){}^{16}\text{O}$ which is also known to be isotropic (Chao 1950; Sanders 1953; Boydell 1973). The last of these measurements was made by bombardment of a TaF_5 target installed in the chamber after completion of the ${}^6\text{Li}(p, \gamma){}^7\text{Be}$ work. The ${}^6\text{Li}(d, p\gamma){}^7\text{Li}$ and ${}^6\text{Li}(d, n\gamma){}^7\text{Be}$ reactions arose from the small deuteron content in the H_2^+ beam. Partial energy level diagrams of ${}^7\text{Li}$ and ${}^7\text{Be}$ are shown in Fig. 2.

3. Results and Analysis

When the target rod was removed it was possible to observe the location of the beam spot: this was 1.5 mm off-centre, to the side away from the angular distribution detector. The variation of detection efficiency with angle was calculated with this displacement being taken into account through its effect on both geometry and thickness of copper traversed by the γ rays. The calculation was carried out for each of the isotropic calibration γ -ray energies, the absorption coefficients being taken from the compilation of Storm and Israel (1970). The experimental raw data are plotted in Fig. 3 and angular distributions based on the calculated relative detection efficiencies are shown as curves. The agreement is excellent and this gave us confidence in the reliability of correcting the ${}^6\text{Li}(p, \gamma){}^7\text{Be}$ angular distribution data by means of the same system of calculation.

The angular distributions for both ${}^6\text{Li}(p, \gamma_0){}^7\text{Be}$ and ${}^6\text{Li}(p, \gamma_1){}^7\text{Be}$ were based on the sum of the counts in the three pair production peaks of the γ rays concerned. The detection efficiency of the Ge(Li) detector for the sum of the three pair production peaks varied as a function of energy by less than 1% over the energy range corresponding to the variation in Doppler shift with angle of observation.

The dominant γ rays in the monitor detector were from the 478 keV $1 \rightarrow 0$ transition in ${}^7\text{Li}$ and the 429 keV $1 \rightarrow 0$ transition in ${}^7\text{Be}$. Since these γ rays were

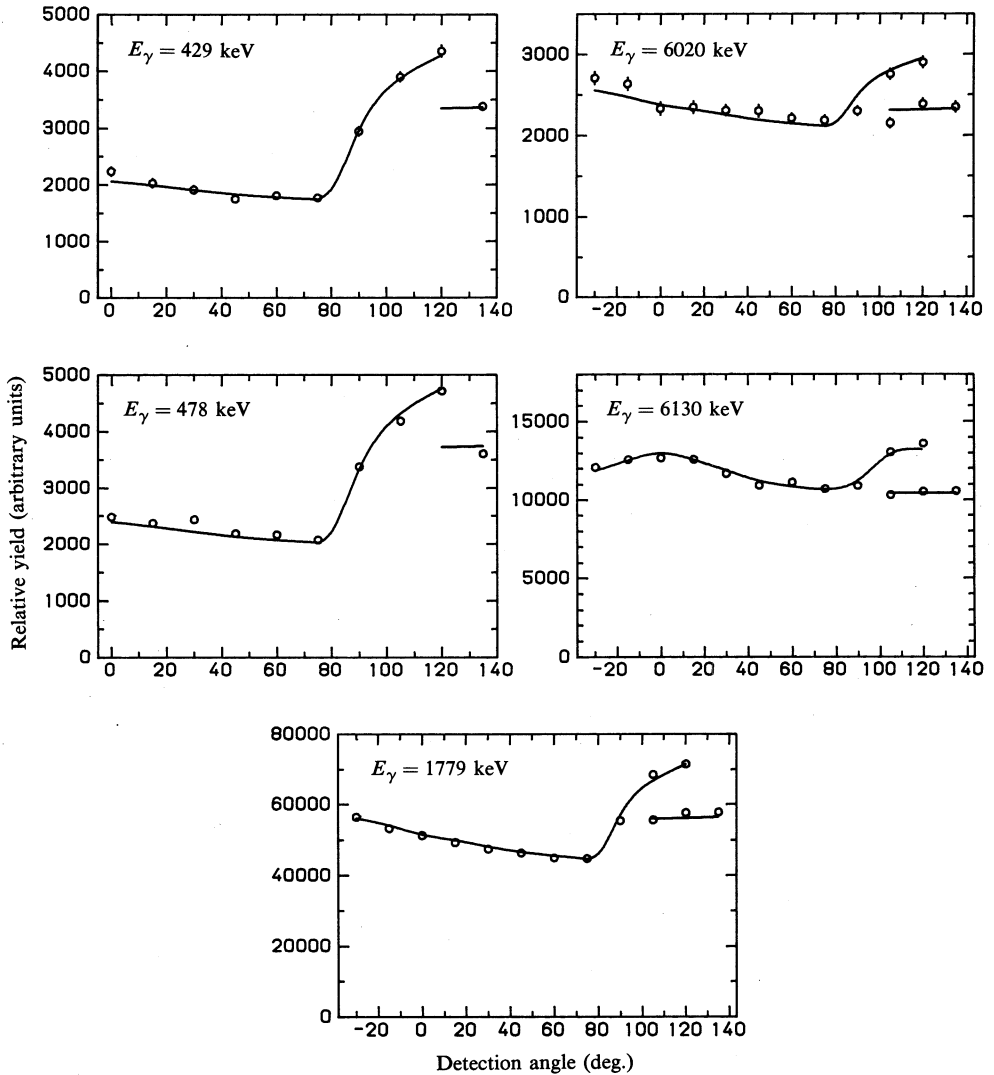


Fig. 3. Comparison of observed relative yields (points) of isotropic γ rays as a function of angle, and those based on calculations (curves) taking into account the effects of absorbers and departures from isotropy in the detection geometry. The low points at back angles represent measurements made with the detector in the 6.2 cm position.

produced not only by ${}^7\text{Li}(p, p'\gamma){}^7\text{Li}$ and ${}^6\text{Li}(p, \gamma){}^7\text{Be}$ but also by ${}^6\text{Li}(d, p\gamma){}^7\text{Li}$ and ${}^6\text{Li}(d, n\gamma){}^7\text{Be}$, for their yield to be a valid monitor for ${}^6\text{Li}(p, \gamma){}^7\text{Be}$ measurements, it was necessary to place upper limits on possible variations with time as a result of variations in the deuteron content of the H_2^+ beam. Since the deuteron content of the beam is a function of ion source conditions, no adjustment was made to any of the ion source controls during any angular distribution measurement. At $E_p = 500$ keV the c.m. energy was below threshold for ${}^7\text{Li}(p, p'\gamma){}^7\text{Li}$, so the yield of 478 keV γ rays was due entirely to ${}^6\text{Li}(d, p\gamma){}^7\text{Li}$. From this yield and the ratio of (d, $n\gamma$) and (d, $p\gamma$) cross sections of McClenahan and Segel (1975), the ${}^6\text{Li}(d, n\gamma){}^7\text{Be}$ contribution to the

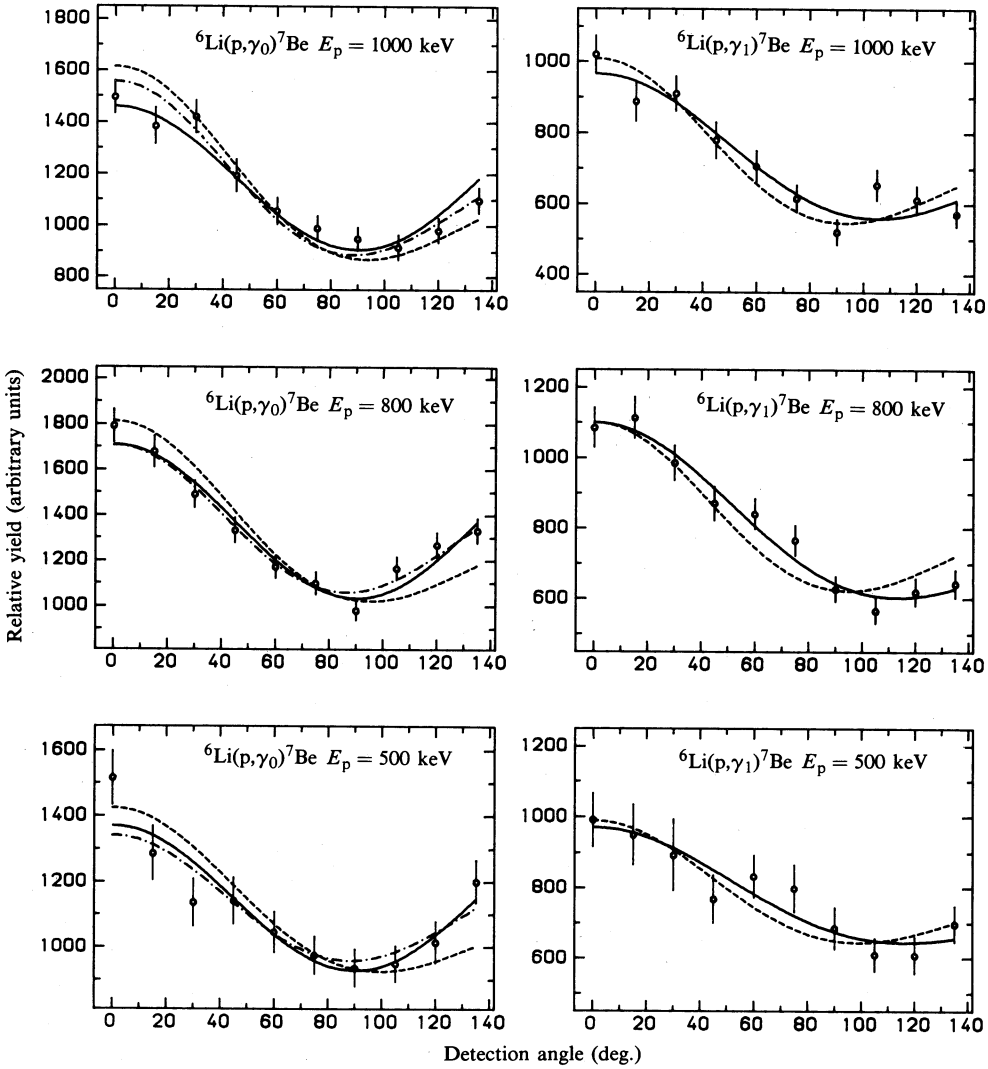


Fig. 4. Angular distributions of γ rays from ${}^6\text{Li}(p, \gamma_0){}^7\text{Be}$ and ${}^6\text{Li}(p, \gamma_1){}^7\text{Be}$. In each case the solid curve is a least squares Legendre polynomial fit to the data, the dashed curve represents the calculation by Barker (personal communication, 1986), and the dot-dash curve corresponds to Barker but with B_1 chosen to optimise the fit.

429 keV γ -ray yield was found to lie in the range $(13 \pm 3)\%$ over the time of the angular distribution measurement. The monitor used was the sum of the 429 keV peak and the six pair production peaks corresponding to ${}^6\text{Li}(p, \gamma_0){}^7\text{Be}$ and ${}^6\text{Li}(p, \gamma_1){}^7\text{Be}$ and, since the 429 keV yield accounted for 80% of the total, the upper limit on monitor variation due to changes of deuteron content of the beam was 2.4%. At $E_p = 800$ keV the monitor consisted of the sum of the 429 and 478 keV peaks and the six pair production peaks. The ${}^6\text{Li}(p, \gamma){}^7\text{Be}$ contribution, and hence the ${}^6\text{Li}(d, n\gamma){}^7\text{Be}$ contribution, to the 429 keV peak was determined from the ${}^6\text{Li}(p, \gamma_1){}^7\text{Be}$ peak and the efficiency calibration of the detector. The ${}^6\text{Li}(d, n\gamma){}^7\text{Be}$ contribution lay in the

range (9±9)% which translated to a ⁶Li(d, pγ)⁷Li contribution to the 478 keV peak in the range (2±2)% and an upper limit of 2.5% on the variation in monitor yield due to variation of the deuteron content of the beam. At $E_p = 1000$ keV, the yield was completely dominated by the 478 keV γ rays. Its peak area was 150 times that of the 429 keV γ ray. An analysis of (d, nγ) and (d, pγ) similar to those used at $E_p = 500$ and 800 keV showed that over 99.5% of the 478 keV yield was due to ⁷Li(p, p'γ)⁷Li and that this peak alone constituted a monitor which was reliable to within 0.25%.

At $E_p = 500$ keV the ⁶Li(p, γ₁)⁷Be full energy and single escape peaks were unresolved from the ¹⁹F(p, αγ)¹⁶O single and double escape peaks, at angles from 0° to 90°. The corrections applied for this contaminant contribution were based on the clearly resolved ¹⁹F full energy peak and the ratios of peak areas for the ¹⁹F γ ray determined from the spectrum obtained with the TaF₃ target. The correction never exceeded 35% on any peak.

The fully corrected angular distribution data are plotted in Fig. 4. The full curves are least squares fits to the data for the function

$$W(\theta) = a \sum_k B_k Q_k P_k(\cos \theta), \quad B_0 = 1,$$

where a is a normalisation constant, the $P_k(\cos \theta)$ are Legendre polynomials, the Q_k are the standard finite solid angle correction factors (Camp and Van Lehn 1969; Krane 1972) corresponding to the solid angle subtended by the detector, and $k = 0, 2$ for (p, γ₀) and $k = 0, 1, 2$ for (p, γ₁). The values of the B_k and chi-squared per degree of freedom for each fit are given in Table 1.

Table 1. Legendre polynomial coefficients for angular distributions

E_p (keV)	⁶ Li(p, γ ₀) ⁷ Be		⁶ Li(p, γ ₁) ⁷ Be		
	B_2	χ^2	B_1	B_2	χ^2
500	0.299±0.045	0.90	0.193±0.055	0.159±0.074	0.78
800	0.390±0.031	1.17	0.283±0.042	0.257±0.051	0.76
1000	0.368±0.036	1.21	0.205±0.043	0.281±0.054	1.67

Table 2. Branching ratios (%) of ⁶Li(p, γ₀) and ⁶Li(p, γ₁) at 0°

Note	$E_p = 500$ keV		$E_p = 800$ keV		$E_p = 1000$ keV	
	(p, γ ₀)	(p, γ ₁)	(p, γ ₀)	(p, γ ₁)	(p, γ ₀)	(p, γ ₁)
A	59±2	41±2	62±2	38±2	61±2	39±2
B			62±5	38±5		
C			62	38		
D			59±3	41±3		

^A Present work. ^B Warren *et al.* (1956). ^C Johnston *et al.* (1969). ^D Switkowski *et al.* (1979).

4. Discussion

Comparison with Other Experimental Data

The ⁶Li(p, γ₀)⁷Be angular distributions reported here show symmetry about 90° and are well fitted by expressions of the form $W(\theta) = B_0 + B_2 P_2(\cos \theta)$. The observed

symmetry about 90° is consistent with the data by Warren *et al.* (1956). The data by Johnston *et al.* (1969) would also be consistent with symmetry about 90° but for one high point, that at their most backward angle of observation, 150° . However, this point could be too high because of an unsuspected yield of 6.13 MeV γ rays from $^{19}\text{F}(p, \alpha\gamma)^{16}\text{O}$ which they would not have resolved from the $^6\text{Li}(p, \gamma_0, \gamma_1)^7\text{Be}$ γ rays with their NaI(Tl) detector. At this backward angle their detector was very close to the tantalum beam-collimator which could have been a significant source of these γ rays and, even with its 10 cm of lead shielding, the detector may have recorded such γ rays in sufficient numbers to distort the low yield $^6\text{Li}(p, \gamma)^7\text{Be}$ measurement. There is therefore no compelling experimental evidence for asymmetry about 90° for $^6\text{Li}(p, \gamma_0)^7\text{Be}$. However, the present $^6\text{Li}(p, \gamma_1)^7\text{Be}$ data are not consistent with symmetry about 90° and the data are well fitted by expressions of the form $W(\theta) = B_0 + B_1 P_1(\cos \theta) + B_2 P_2(\cos \theta)$. This asymmetry about 90° for (p, γ_1) coupled with symmetry for (p, γ_0) is at variance with the work of both Warren *et al.* and Johnston *et al.* who reported a ratio of γ_0 and γ_1 which was independent of angle. However, we are in agreement with all authors with respect to the value of this ratio at 0° and 800 keV, and with the finding by Warren *et al.* that this ratio does not depend on energy. The comparisons are made in Table 2.

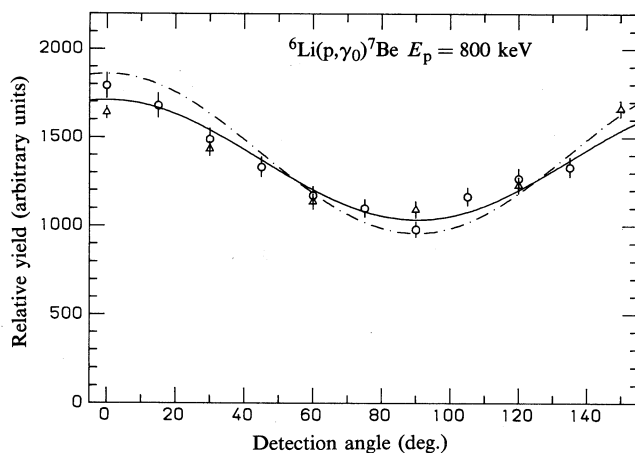


Fig. 5. Comparison of the experimental results of the present work (circles), of Johnston *et al.* (1969) (triangles), and of Warren *et al.* (1956) (dot-dash curve). The solid curve is the least squares Legendre polynomial fit to the present data.

Overall, there is a fair level of agreement among all the experimental (p, γ_0) angular distribution data, as illustrated in Fig. 5. Here, in addition to our own data (circles), we have plotted the data by Johnston *et al.* (triangles). Warren *et al.* did not publish their data, giving only a best fit expression $W(\theta) = 1 + (1.05 \pm 0.15) \cos^2 \theta$ which we have reproduced as the dot-dash curve. Our least squares fit is given by the solid curve. To make the comparisons with our data valid, we have adjusted the data points and curves of the other authors with the Q_k factors corresponding to the finite

solid angle corrections applicable to our experiment. There are no published explicit (p, γ_1) angular distribution data with which to compare our results.

Comparison with Theory

Of the nine parameter sets considered by Barker (1980), only three gave satisfactory agreement with our (p, γ_1) angular distributions. One of these introduced a hard core in all nuclear potentials, another introduced a cut-off radius in the radial integral, and the third introduced a nuclear radius 35% greater than that used in his standard parameter set. The set involving the hard core was also one of the two sets which gave the overall best fit to the cross-section data tabulated by Barker for ${}^6\text{Li}(p, \gamma){}^7\text{Be}$ and the mirror reaction ${}^6\text{Li}(n, \gamma){}^7\text{Li}$. We therefore limit our discussion to comparisons with this particular model, the angular distributions from which are shown in Fig. 4 as the dashed curves. Barker (1980) gave Legendre polynomial coefficients only for ${}^6\text{Li}(p, \gamma_0){}^7\text{Be}$ at $E_p = 800$ keV, and the angular distributions shown in Fig. 4 are based on coefficients provided by Barker (personal communication, 1986). The remaining five parameter sets gave fits with chi-squared values greater than those for the chosen set, at all three energies, and greater by a factor between 1.5 and 2.5 at at least one energy.

Table 3. Legendre polynomial coefficients for theoretical angular distributions

E_p (keV)	Note	${}^6\text{Li}(p, \gamma_0){}^7\text{Be}$				${}^6\text{Li}(p, \gamma_1){}^7\text{Be}$			
		B_1	B_2	B_3	χ^2	B_1	B_2	B_3	χ^2
500	A	0.135	0.229	0.030	3.05	0.130	0.229	0.030	1.35
	B	0.017	0.229	0.030	1.43				
800	A	0.155	0.329	0.059	5.58	0.148	0.330	0.058	3.39
	B	0.013	0.329	0.059	1.19				
1000	A	0.156	0.360	0.078	2.91	0.148	0.359	0.076	2.51
	B	0.069	0.360	0.078	1.56				

^A All coefficients are from Barker (personal communication, 1986).

^B Coefficients B_2 and B_3 are from Barker (personal communication, 1986), with B_1 chosen to optimise the fit.

Whilst the theoretical model gave satisfactory agreement with the observed (p, γ_1) angular distributions, the agreement with the (p, γ_0) data is not as good. However, for the ${}^7\text{Li}(\gamma, n_0){}^6\text{Li}$ inverse mirror reaction, Barker included an M1 resonant contribution from the $\frac{5}{2}^-$ level in ${}^7\text{Li}$ at 7.46 MeV in addition to direct capture. If a similar M1 contribution is included in the ${}^6\text{Li}(p, \gamma){}^7\text{Be}$ calculation by way of the $\frac{5}{2}^-$ analogue level in ${}^7\text{Be}$ at 7.21 MeV, it will influence the (p, γ_0) angular distributions but not those for (p, γ_1) to the $\frac{1}{2}^-$ first excited state of ${}^7\text{Be}$. The effect on the (p, γ_0) angular distributions is expected to be seen mainly in B_1 , the coefficient of $P_1(\cos \theta)$ (Barker, personal communication, 1986). We have accordingly obtained least squares fits to the data by taking Barker's B_2 and B_3 values and treating B_1 as a free parameter. The results are shown as the dot-dash curves in Fig. 4. The agreement with the experimental data is good. The Legendre polynomial coefficients for all the theoretical curves in Fig. 4 are listed in Table 3 together with chi-squared for the fits to the data. From these results it is clear that any reduction in B_1 will improve the (p, γ_0) theoretical fit and that, if inclusion of the M1 resonant contribution of the $\frac{5}{2}^-$ level

brings about such a reduction, Barker's hard core nuclear potential model will be in substantial agreement with all the experimental data.

The remaining small difference between our angular distribution data and the predictions of the model would then be attributable to the nonzero value of B_3 in the theory. We investigated the effect of including $P_3(\cos \theta)$ in our least squares fitting procedures and obtained negligibly small values of B_3 for both (p, γ_0) and (p, γ_1) , and no improvement in chi-squared. We therefore conclude that any further variation of the model parameters which will reduce B_3 , without simultaneously reducing B_2 , would bring the model into even better agreement with experiment.

Acknowledgments

We are indebted to Dr F. C. Barker for his careful and critical reading of the manuscript which resulted in significant alterations and improvement to the text, and for supplying us with his unpublished angular distribution coefficients.

References

- Ajzenberg-Selove, F. (1984). *Nucl. Phys. A* **413**, 1.
- Anttila, A., Keinonen, J., Hautala, M., and Forsblom, I. (1977). *Nucl. Instrum. Methods* **147**, 501.
- Barker, F. C. (1974). Fifth AINSE Nuclear Physics Conf., Canberra 1974, Abstracts p. 36 (Aust. Nat. Univ.).
- Barker, F. C. (1980). *Aust. J. Phys.* **33**, 159.
- Boydell, S. G. (1973). Ph.D. Thesis, Univ. of Melbourne.
- Camp, D. C., and Van Lehn, A. L. (1969). *Nucl. Instrum. Methods* **76**, 192.
- Chao, C. Y. (1950). *Phys. Rev.* **80**, 1035.
- Johnston, G. P., Switkowski, Z. E., and Sargood, D. G. (1969). Int. Conf. on Properties of Nuclear States, Montreal, p. 272 (Univ. Montreal Press).
- Krane, K. S. (1972). *Nucl. Instrum. Methods* **98**, 205.
- McClenahan, C. R., and Segel, R. E. (1975). *Phys. Rev. C* **11**, 370.
- Sanders, J. E. (1953). *Philos. Mag.* **44**, 1302.
- Storm, E., and Israel, H. I. (1970). *Nucl. Data Tables A* **7**, 565.
- Switkowski, Z. E., Heggie, J. C. P., Kennedy, D. L., Sargood, D. G., Barker, F. C., and Spear, R. H. (1979). *Nucl. Phys. A* **331**, 50.
- Warren, J. B., Alexander, T. K., and Chadwick, G. B. (1956). *Phys. Rev.* **101**, 242.